https://doi.org/10.5194/egusphere-2023-1292
Preprint. Discussion started: 14 June 2023

Spatial and Diurnal Variations of Aerosol Organosulfates in Summertime Shanghai, China: Potential Influence of Photochemical Process and Anthropogenic Sulfate Pollution

Ting Yang[1], Yu Xu[1,*], Qing Ye[1], Yi-Jia Ma[1], Yu-Chen Wang[2], Jian-Zhen Yu[2], Yu-Sen Duan[3], Chen-Xi Li[1], Hong-Wei Xiao[1], Zi-Yue Li[1], Yue Zhao[1,*], Hua-Yun Xiao[1,*]

[1]School of Environmental Science and Engineering, Shanghai Jiao Tong University, Shanghai 200240, China

[2]Division of Environment & Sustainability, Hong Kong University of Science & Technology, Hong Kong SAR, China

[3]Shanghai Environmental Monitoring Center, Shanghai 200235, China

*Corresponding authors

Yu Xu, e-mail: xuyu360@sjtu.edu.cn

Yue Zhao, e-mail: yuezhao20@sjtu.edu.cn

Hua-Yun Xiao, e-mail: xiaohuayun@sjtu.edu.cn

https://doi.org/10.5194/egusphere-2023-1292
Preprint. Discussion started: 14 June 2023

ABSTRACT： Organosulfates (OSs) are ubiquitous aerosol components with intense research over years. However, spatial and diurnal variations in OS formation in polluted atmosphere remain poorly understood. In this study, 130 OS species were quantified in ambient fine particulate matter ($PM_{2.5}$) collected in urban and suburban Shanghai (East China) in summer 2021. Isoprene- and monoterpene-derived OSs were dominant OS groups (averaging 51% and 19% of total quantified OSs, respectively), likely indicating a large biogenic contribution to OS formation in summer. Most OSs peaked during daytime, while monoterpene-derived nitrooxy-OSs (NOS_m) increased during nighttime. Accordingly, OSs were largely produced via daytime formation processes, rather than nighttime chemistry, excepting NOS_m. Additionally, although OS formation in the urban and suburban areas exhibited similar diurnal variations, the average concentrations of biogenic and anthropogenic OSs decreased significantly from the urban site to the suburban site. Furthermore, we concretized daytime OS formation based on the interactions among OSs, ultraviolet (UV), ozone (O_3), and sulfate (SO_4^{2-}). Indeed, the concentrations of most OSs were significantly correlated with the values of $UV[O_3][SO_4^{2-}]$ during daytime in both urban and suburban Shanghai. In particular, the correlation between major OSs and $UV[O_3][SO_4^{2-}]$ was stronger than the correlation of major OSs with O_3 and SO_4^{2-}; moreover, there was no significant correlation between major OSs and UV. Thus, higher urban OS events were attributed to the enhanced photochemical processes and sulfate level in the urban area. Overall, this study provides field evidence for the influence of photochemical process and anthropogenic sulfate on OS formation and has important implications for the mitigation of organic particulate

https://doi.org/10.5194/egusphere-2023-1292
Preprint. Discussion started: 14 June 2023

pollution.

KEYWORDS: Organosulfates; Aerosols; Photooxidation; Sulfate pollution; Shanghai

1. Introduction

Organosulfates (OSs) are ubiquitous constituents in secondary organic aerosol (SOA) and can contribute up to ~30% of organic mass in atmospheric fine particles ($PM_{2.5}$) (Tolocka and Turpin 2012; Stone et al. 2012; Surratt et al. 2008). OSs affect the formation, hygroscopicity, light-absorbing, and acidity of organic aerosols as well as biogeochemical cycles of sulfur (Estillore et al. 2016; Riva et al. 2019; Fleming et al. 2019), which are tightly associated with air quality, human health, and regional climate (Ramanathan et al. 2001; Menon et al. 2008). Thus, understanding the mechanisms and key influencing factors of OS formation in the ambient atmosphere is of great significance for an effective assessment of environment and climate effects of OSs.

Many laboratory studies have suggested that heterogeneous and multiphase reactions involving biogenic and anthropogenic volatile organic compounds (VOCs), their oxidation intermediates, and sulfate or gas-phase sulfur dioxide (SO_2) are important pathways for the formation of OSs (Blair et al. 2017; Riva et al. 2016b; Ye et al. 2018). For example, the formation of 2-methyltetrol sulfate ester (2-MT-OS) and 2-methylglyceric acid sulfate ester (2-MGA-OS) can be attributed to the reactive uptake of isoprene epoxydiols (IEPOX) and isoprene-derived hydroxymethel-methyl-α-lactone (HMML) by acidic particles, respectively (Surratt et al. 2010; Nguyen et al. 2015). The ozonolysis of α-pinene and limonene in the presence of SO_2 can contribute

https://doi.org/10.5194/egusphere-2023-1292
Preprint. Discussion started: 14 June 2023

to the production of monoterpene-derived OSs (e.g., $C_9H_{15}O_7S^-$ and $C_{10}H_{17}O_7S^-$) (Ye et al. 2018). Chamber experiments by Riva et al., (2015) showed that the photooxidation of C_{10}–C_{12} alkanes is associated with the formation of aliphatic OSs. More recently, the aliphatic OSs have been identified based on the uptake experiments of SO_2 by oleic acid and other unsaturated fatty acids (Shang et al. 2016; Passananti et al. 2016). In addition, the gas-phase oxidation of polycyclic aromatic hydrocarbons was found to be an important source of aromatic OSs (Riva et al. 2015).

Furthermore, OSs have been identified in different ambient atmospheres, including suburban, rural, urban, marine, polar, and forest areas (Kristensen and Glasius 2011; Tao et al. 2014; Hettiyadura et al. 2017; Vandergrift et al. 2022; Hawkins et al. 2010; Ye et al. 2021). Owing to different levels of precursors and atmospheric pollution, the abundance and formation pathways of OSs change substantially in temporal and spatial scales (Lin et al. 2022; Wang et al. 2021). Patently, field observations are valuable for verifying the mechanistic understanding of OS formation obtained in the laboratory studies. The importance of atmospheric oxidants and sulfate (or SO_2) in the OS formation was proposed in field observations according to a correlation analysis of OSs with ozone (O_3) (or the sum of O_3 and NO_2 concentrations) and sulfate (or SO_2) (Nguyen et al. 2014; Hettiyadura et al. 2019; Wang et al. 2018). Notably, these observation-based studies also highlighted the role of photochemistry of OS precursors. However, the interactions among ultraviolet (UV), O_3, and sulfate have not been well investigated. In particular, few studies were performed to systematically reveal the difference in the formation processes of OSs in polluted and clean areas, as well as

https://doi.org/10.5194/egusphere-2023-1292
Preprint. Discussion started: 14 June 2023

during daytime and nighttime.

Shanghai is a megacity in the Yangtze River Delta (YRD) region of China. Locally varied ambient conditions such as O_3, SO_2, and NO_x, relative humidity (RH), and aerosol acidity affect the formation of OSs significantly (Cai et al. 2020; Wang et al. 2021). Here, 130 OS species were quantified in $PM_{2.5}$ samples collected in urban and suburban Shanghai in summer 2021 to investigate the relative influence of photochemistry and nighttime chemistry on OS formation and their linkages with anthropogenic sulfate pollution. In addition, the potential impacts of aerosol acidity and aerosol liquid water (ALW) on OS formation were discussed. This study can help to deepen the understanding of photochemical process and nighttime chemistry of OSs in the atmosphere.

2. Materials and Methods

2.1 Site Description and Sample Collection

Ambient $PM_{2.5}$ samples were continuously collected in the urban center and suburban area in Shanghai from 11 to 23 July 2021 (**Figure S1**). The sampling site in the urban center is located on the roof of a building (~20 m above the ground) in the Xuhui Campus of Shanghai Jiao Tong University. The site is characterized by a typical urban environment with heavy traffic and dense population. The aerosol sampler in the suburban area was placed on the roof of a ~20 m high building in a monitoring station of Pudong Huinan. This site is closer to the coastline than the urban sampling site (**Figure S1**). Thus, the suburban site is expected to be more affected by clean air mass

https://doi.org/10.5194/egusphere-2023-1292
Preprint. Discussion started: 14 June 2023

from the sea. $PM_{2.5}$ was sampled onto the prebaked (550°C for ~8 h) quartz fiber filters (8 × 10 in., Whatman) using a high-volume air sampler (HiVol 3000, Ecotech) at a flow rate of 67.8 m^3 min^{-1}. The duration of each sample collection in both urban and suburban areas was approximately 11 h during the daytime (8:30−19:30 LT) and 12 h during the nighttime (20:00−8:00 LT). Two blank filter samples were collected at each site during the campaign. A total of 50 filter samples were collected, which were stored at −30°C until analysis.

2.2 Chemical Analysis and Prediction of Aerosol Acidity and ALW

A portion of the filter (~15.9 cm^2) was extracted with 3 mL methanol in an ultrasonic bath for 30 min for two times. The camphorsulfonic acid (1 ppm) was spiked on the filter punches as an internal standard before extracting. The extracts obtained each time were combined and filtered through a 0.22 μm Teflon syringe filter (CNW Technologies GmbH) and then concentrated to 300 μL under a gentle stream of ultra-high-purity nitrogen gas. Subsequently, 300 μL ultrapure water was added into the concentrated samples, followed by centrifugation to get the supernatant for analysis. OSs were analyzed using an Acquity UPLC (Waters, USA) coupled to a Xevo G2-XS Qudropole time-of-flight mass spectrometer (ToF-MS, Waters, USA) equipped with an electrospray ionization (ESI) source operated in the negative ion mode. The chromatographic conditions and analytical procedures were detailed in our recent publication (Wang et al. 2021). A total of 212 OSs were identified by UPLC-MS analysis, in which 130 OS species were quantified (**Table 1** and **Table S1**). The

https://doi.org/10.5194/egusphere-2023-1292
Preprint. Discussion started: 14 June 2023

quantified species included isoprene-derived OSs (OS_i), monoterpene-derived OSs (OS_m), C_2-C_3 OSs, aliphatic OSs, and aromatic OSs (Hettiyadura et al. 2019). The recoveries of OS standards ranged from 84% to 94%. Detailed data quality control was described in our recent publication (Wang et al. 2021). In addition, more details about the classification and quantification of OSs were described in the Supplementary Information (**Sect. S1**) and **Table S1**.

The mass concentrations of organic carbon (OC) and elemental carbon (EC) were determined via an OC/EC analyzer (DRI Model 2015). The mass concentrations of OC were converted to those of organic matter (OM) using a conversion factor of 1.6 (Turpin and Lim 2001; Wang et al. 2021; Wang et al. 2018). The mass concentrations of inorganic ions in $PM_{2.5}$ samples, including Na^+, NH_4^+, K^+, Mg^{2+}, Ca^{2+}, Cl^-, NO_3^-, and SO_4^{2-}, were measured using an ion chromatograph system (ICS-5000+, Thermo, USA).

A thermodynamic model (ISORROPIA-II) was used to predict the mass concentration of ALW and pH (Guo et al. 2015; Hennigan et al. 2015). The model was operated with particle-phase concentrations of Na^+, SO_4^{2-}, NH_4^+, NO_3^-, Cl^-, Ca^{2+}, K^+, and Mg^{2+}, as well as ambient temperature (T) and RH as the inputs. Moreover, the forward mode with the thermodynamically metastable state was selected. The detailed descriptions on ALW and pH predictions were shown in our previous studies (Wang et al. 2021; Xu et al. 2020).

2.3. Auxiliary Data and Data Analysis

The transport trajectories of air masses arriving at the sampling sites during the

https://doi.org/10.5194/egusphere-2023-1292
Preprint. Discussion started: 14 June 2023

sampling period were created using the database of NOAA's Air Resources Laboratory (NOAA's Air Resources Laboratory, USA) and MeteoInfoMap software coupled with TrajStat program (Chinese Academy of Meteorological Sciences, China). The data of T, RH, wind speed, and UV irradiation as well as the concentrations of NO, NO_2, O_3, SO_2, and $PM_{2.5}$ at the urban and suburban sites were obtained from the environmental monitoring stations of Xuhui (~4 km away from the sampling site) and Pudong Huinan (~10 m away from the sampling site), respectively. The ventilation coefficient (VC) can be used to characterize the state of atmospheric dilution in pollutant concentrations (Gani et al. 2019). The VC value can be expressed as a product of wind speed and planetary boundary layer height (PBLH).

3. Results and Discussion

3.1. Molecular compositions and concentrations of OSs

The mass concentrations and mass fractions of the OS species in $PM_{2.5}$ collected in Shanghai were shown in **Figure 1**, with a focus on their spatial and diurnal differences. On average, isoprene-derived OSs (i.e., OS_i) were the dominant components at both urban and suburban sites (**Figures 1a**,**d**), which accounted for 53.9 ± 0.1% and 48.1 ± 0.1% of the total OS masses, respectively. The mass fractions and concentrations of $C_5H_{11}O_7S^-$ were the highest among all kinds of OS_i. In contrast, OS_i containing nitrogen atoms only accounted for a small proportion of OS_i in both urban and suburban areas (**Figures 1a,d** and **Table S2**). Monoterpene-derived OSs (OS_m) were the second most abundant OS components, whose concentrations averaged 30.6

https://doi.org/10.5194/egusphere-2023-1292
Preprint. Discussion started: 14 June 2023

± 46.4 ng m^{-3} and 19.3 ± 25.7 ng m^{-3} in the urban and suburban areas, respectively. Moreover, the abundance of OS_m was also less controlled by nitrogen-containing OS_m. On average, the OS species with two or three carbon atoms (C_2-C_3 OSs) and anthropogenic OSs (OS_a) together contributed to 26.8% and 33.1% of total OS concentrations in the urban and suburban areas, respectively (**Figures 1a,d** and **Table S3**). A similar pattern in the relative abundance of different groups of OSs was also observed at the same sites in summer 2020 (**Figure S2**). The predominance of OS_i was well documented by many previous observations in Beijing, China (Wang et al. 2018), Guangzhou, China (Bryant et al. 2021), and Atlanta, Georgia, USA (Hettiyadura et al. 2019), Hong Kong, China (Wang et al. 2022), Copenhagen, Denmark (Nguyen et al. 2014), Centreville, AL, USA (Hettiyadura et al. 2017), Zion, Illinois, USA (Hughes et al. 2021). A reasonable explanation for these cases is that there is a large biogenic emission of isoprene, particularly during summer days with higher temperature than in other seasons (Bryant et al. 2021). Interestingly, we found that the mass concentrations of all types of OSs (i.e., total OS_i, OS_m, C_2-C_3 OSs, and OS_a) tended to decrease from the urban area to the suburban area. This spatial difference in OS concentrations can be attributed to varied atmospheric oxidation capacity and aerosol properties (e.g., sulfate, acidity, and ALW) (Wang et al. 2021), which will be discussed in detail below.

Table S4 gives an overview of OSs in $PM_{2.5}$ in different regions around the world. The concentrations of total OSs in our study (more than 102.3 ng m^{-3}) were higher than those in Copenhagen, Denmark (75.7 ng m^{-3}) (Nguyen et al. 2014), and Beijing, China (27.4 ng m^{-3}) (Wang et al. 2018). However, the OSs showed a lower concentration in

https://doi.org/10.5194/egusphere-2023-1292
Preprint. Discussion started: 14 June 2023

Shanghai compared to the observations in Guangzhou (486.4 ng m^{-3}) (Wang et al. 2022) and Atlanta, USA (Hettiyadura et al. 2019) (1249.4 ng m^{-3}). The concentrations of OS_i in this study were lower than those observed in summertime Atlanta, USA (1123.0 ng m^{-3}) (Hettiyadura et al. 2019), Guangzhou, China (460.2 ng m^{-3}) (Wang et al. 2022), and Hongkong, China (163.2 ng m^{-3}) (Wang et al. 2022), but higher than Copenhagen, Denmark (11.3 ng m^{-3}) (Nguyen et al. 2014). For OS_m and C_2-C_3 OSs, their concentrations also showed a variable rang in different regions (**Table S4**). The concentrations of OS_a in this study were much higher than those in previous observations (Hettiyadura et al. 2017; Kanellopoulos et al. 2022), which is likely explained by more OS_a species being quantified or higher air pollution level in this study. In general, the abundances of OS_i and OS_m were higher than those of other quantified OSs in summer (**Table S4**). Thus, the yield of summertime OSs in different regions largely depends on the emission level of biogenic VOCs and the air pollution status.

We found that the contributions of total OSs to OM were 1.3 ± 0.5% and 1.9 ± 0.5% at urban and suburban sites in summer 2021, respectively. These proportions of total OSs in OM were larger than those observed in Beijing, China (0.3%) (Wang et al. 2018) and Centreville, USA (0.2%) (Hettiyadura et al. 2017). However, significant higher contribution of total OSs to OM was observed in Atlanta, USA (10.3%) (Hettiyadura et al. 2019) where the formation of OSs was dominated by the oxidation of biogenic VOCs. In particular, total OSs contributed to 1.2 ± 0.8% of OM in summer 2015 and 1.1 ± 0.8% of OM in summer 2019 in urban Shanghai (Wang et al. 2021). Thus, although anthropogenic emission reduction has been vigorously promoted by the local

https://doi.org/10.5194/egusphere-2023-1292
Preprint. Discussion started: 14 June 2023

government in recent years, the contribution of SOA to OM in Shanghai has not decreased significantly as expected.

Figures 1b,e show diurnal differences in the mass concentrations and mass fractions of the OS components in $PM_{2.5}$ collected at the urban site. The OS_i was the dominant sulfur-containing species regardless of in daytime and nighttime. However, the concentrations of OS_i exhibited a significant decrease from the daytime (117.8 ± 148.1 ng m^{-3}) to the nighttime (43.9 ± 62.0 ng m^{-3}), except for isoprene-derived nitrooxyorganosulfates (NOS_i). Moreover, the variations in OS_i mass concentrations (~2 times) were much larger than those in OS_i mass fractions (< 1.2 times). These results indicate that the production of major OS_i (e.g., $C_5H_{11}O_7S^-$, $C_5H_9O_7S^-$ and $C_5H_7O_7S^-$) was weakened during the nighttime. In contrast, the higher concentration for these OS_i in the daytime can be attributed to the increased levels of precursors (e.g., isoprene) (Bryant et al. 2021) and oxidants (e.g., O_3) (**Table S5**) as well as the strong photochemistry in the daytime. Although the average fraction of NOS_i was higher in the nighttime than in the daytime, their concentration was similar between the daytime and nighttime. This is because that several special NOS_i (e.g., $C_5H_{10}NO_9S^-$, $C_5H_8NO_{10}S^-$, $C_4H_8NO_7S^-$, and $C_5H_8NO_7S^-$) peaked in the daytime, although $C_5H_9N_2O_{11}S^-$ showed maximum in the nighttime (**Table S2**). Previous laboratory studies have suggested that the formation of $C_5H_{10}NO_9S^-$ is mainly related to •OH oxidation processes (Hamilton et al. 2021). Thus, a strong photochemical oxidation during daytime can be responsible for the increases in concentrations of these NOS_i (particularly $C_5H_{10}NO_9S^-$) from the nighttime to the daytime. Overall, the diurnal

https://doi.org/10.5194/egusphere-2023-1292
Preprint. Discussion started: 14 June 2023

variations of other OSs including OS_m, C_2-C_3 OSs, and OS_a were similar to that of OS_i, with a higher level in the daytime than in the nighttime excepting for NOSs (**Figure 1** and **Tables S2** and **S3**). It is noteworthy that the fractions and concentrations of monoterpene-derived NOSs (NOS_m) were higher in the nighttime than in the daytime (**Table S2**). This case can be attributed to NO_3•-related nighttime chemistry (Wang et al. 2018). Thus, these findings further emphasize the importance of photochemistry for daytime OS formation and nighttime chemistry for NOS (in particular NOS_m) formation in urban Shanghai.

The concentrations of various types of OSs at the suburban site were lower than those at the urban site in both daytime and nighttime (**Figures 1e,f**). However, the characteristics of diurnal difference in various OSs at the suburban site were similar to those observed at the urban site, which showed a substantially higher OS level in the daytime. A similar case was also found in Beijing in 2016 (Wang et al. 2018) and Shanghai in 2017 (Cai et al. 2020). Clearly, the aerosol OS abundance in Shanghai was mainly controlled by the OS formation process in the daytime rather than in the nighttime.

3.2. Time series of the major OSs

Figures 2a-2h compare the time series of the major OS species and inorganic ions in $PM_{2.5}$ collected at urban and suburban sites. The OS_i concentrations peaked during daytime on July 11 and 12, with maximum values of 479.8 ng m^{-3} and 309.5 ng m^{-3} at urban and suburban sites, respectively. Owing to the high proportion of OS_i in total OSs,

https://doi.org/10.5194/egusphere-2023-1292
Preprint. Discussion started: 14 June 2023

total OS concentrations also showed maximum values during July 11 and 12. The mass concentrations of total OSs, OS_i, and $C_5H_{11}O_7S^-$ (a major OS_i component) decreased from July 11 to July 14 (period A; i.e., relatively polluted period) in both urban and suburban areas, whereas their concentrations exhibited a quite small fluctuation after July 14 (period B; i.e., clean period). As a result, the mean concentrations of total OSs and OS_i were ~4 times higher in the period A than in the period B. The temporal variations in the concentrations of OS_m, $C_8H_{13}O_7S^-$ (a major component of OS_m) (Schindelka et al. 2013), OS_a, and C_2-C_3 OSs were similar to those of total OSs and OS_i. However, the dissimilarities in the diurnal variations of OSs in period A and period B suggest that the sources or levels of precursors and oxidants associated with OS formation differed between these two periods. This consideration was further supported by decreasing O_3 and NO_2 levels from period A to period B (**Table S5** and **Figures 2i,j**).

Sulfate showed a temporal variation similar to total OSs, OS_i, and OS_m concentrations in most days (**Figures 2g,h**). We observed several abnormally high sulfate events during period B (from the evening of the 17th to 18th). The transport distance of air mass on July 18 was found to be shorter than that in other days (**Figure S3**); moreover, VC value was lower on July 18 than on other days (**Figure S4**). Thus, this high sulfate case can be partly attributed to the special meteorological conditions on July 18. In general, sulfate concentrations showed a strong correlation with total OSs, OS_i, and OS_m concentrations at both sites ($P < 0.01$, $r = 0.76$–0.78). These results indicate that the abundances of OSs in these two study areas were tightly associated with sulfate-related particle-phase chemistry (Surratt et al. 2008).

https://doi.org/10.5194/egusphere-2023-1292
Preprint. Discussion started: 14 June 2023

The concentrations of total OSs, OS_i, and OS_m exhibited a distinct diurnal variation during period A at both sites, with a higher concentration in the daytime. The diurnal variation pattern of OSs was similar to those of O_3 and sulfate. These findings imply an important role of atmospheric oxidation capacity and sulfate in daytime OS formation. Exceptionally, although a clear diurnal pattern was also observed for NOS_m, their concentrations peaked in the nighttime, suggesting that the formation of NOS_m was highly affected by the NO_3•-related nighttime chemistry (Iinuma et al. 2007; Surratt et al. 2008). In the period B, the concentrations of various OSs showed a weak diurnal variation, with a slightly higher level in the daytime.

As mentioned above, the ambient levels of oxidants (e.g, O_3 and NO_2) and sulfates showed a significant difference in period A and period B, which were tightly associated with the formation of OSs (Wang et al. 2021). Cluster analysis of backward trajectories showed that air masses arriving at both urban and suburban sites in the period A mainly originated from the continental region, with significant influences of anthropogenic emissions (e.g., NO_x and SO_2) from southern YRD. Furthermore, considering the distinct and similar diurnal variation of O_3, NO_2, SO_2, sulfate, and OSs during period A at both sites, aerosol OSs can be assumed to be mainly formed in local areas. In contrast, these two sampling sites were primarily affected by air masses transported from the East China Sea in the period B. Moreover, the average VC value in the period A was two times lower than that in the period B (**Table S5**), implying relatively weaker diffusion and dilution of air pollutants in the period A. These factors can be partly responsible for the higher oxidant and sulfate concentrations in the period A than in the

https://doi.org/10.5194/egusphere-2023-1292
Preprint. Discussion started: 14 June 2023

period B. Similarly, since the suburban site is closer to the East China Sea with a decreased influence from anthropogenic emissions (**Figure 3**), the levels of O_3, NO_x, and sulfate were higher at the urban site than at the suburban site (**Figure 2** and **Table S5**). The differences in the concentration of oxidants and sulfate might provide an explanation for the difference in the concentrations of OSs between periods A and B as well as between urban and suburban sites.

3.3. Formation mechanisms of OSs

3.3.1 Isoprene-derived OSs

Previous laboratory studies have suggested that isoprene can react with •OH to form IEPOX in the gas phase under low NO_x conditions (Fabien et al. 2009). In the daytime, ambient O_3 can be rapidly photolyzed to generate •OH under the influence of UV (Kourtchev et al. 2015). Thus, O_3 and UV could serve as a proxy of •OH. Considering a significant role of photochemistry and sulfate-related heterogeneous chemistry in the formation of OSs, OS_i production is expected to be closely associated with isoprene, O_3, UV, and sulfate. Specifically, the simplified pathways leading to the formation of OS_i in the atmosphere can be derived as follows.

$$O_3 + h\nu \rightarrow O(^1D) + O_2 \qquad J_{O_3} \qquad (1)$$

$$O(^1D) + H_2O \rightarrow 2\ \bullet OH \qquad k_1 \qquad (2)$$

$$O(^1D) + M \rightarrow O(^3P) + M \qquad k_2 \qquad (3)$$

$$\text{Isoprene} + \bullet OH \rightarrow X \qquad k_3 \qquad (4)$$

$$X + SO_4^{2-} \rightarrow OS_i \qquad k_4 \qquad (5)$$

https://doi.org/10.5194/egusphere-2023-1292
Preprint. Discussion started: 14 June 2023

Where J_{O_3} is the photolysis rate constant, k_{1-4} is the second-order rate coefficient, M is N_2 or O_2, and X represents the potential products (e.g., IEPOX and HMML) of isoprene oxidation by •OH.

Assuming the concentrations of $O(^1D)$ and •OH are in the steady state, we can derive the following equations (Seinfeld and Pandis, 2016).

$$[O(^1D)] = \frac{J_{O_3}[O_3]}{k_1[H_2O] + k_2[M]} \quad (6)$$

$$[\bullet OH] = 2\tau_{OH}k_1[O(^1D)][H_2O] \quad (7)$$

Where τ_{OH} is the average lifetime of •OH. In general, J_{O_3} is linearly dependent on the UV radiation, i.e., $J_{O_3} = \varphi UV$, where φ is the slope of the linear fitting between J_{O_3} and UV radiation (Li et al. 2022). Combining equation (6) and (7), the steady-state •OH concentration can be expressed as:

$$[\bullet OH] = \frac{2\tau_{OH}k_1[H_2O]\,J_{O_3}[O_3]}{k_1[H_2O] + k_2[M]} = \alpha\varphi\tau_{OH}UV[O_3] \quad (8)$$

$$\alpha = \frac{2k_1[H_2O]}{k_1[H_2O] + k_2[M]} \quad (9)$$

Also, assuming a steady-state to the oxygenated organic intermediates (i.e., X), we can derive:

$$[X] = k_3\tau_X[Isoprene][OH] = \alpha\varphi k_3\tau_X\tau_{OH}[Isoprene]UV[O_3] \quad (10)$$

Where τ_X is the average lifetime of X in the atmosphere.

During the strong formation of OS_i via the heterogeneous reactions of X on acidic sulfate, the change in the abundance of OS_i is expected to be proportional to its formation rate:

$$\frac{d[OS_i]}{dt} \propto k_4[SO_4^{2-}][X] \propto \alpha\varphi k_3k_4\tau_X\tau_{OH}[Isoprene]UV[O_3][SO_4^{2-}] \quad (11)$$

It should be noted that the above equations are derived based on the assumption

https://doi.org/10.5194/egusphere-2023-1292
Preprint. Discussion started: 14 June 2023

that the reaction between $O(^1D)$ and H_2O is a major source of summertime •OH in the studied areas. Given that a linear relationship was observed between atmospheric •OH and $J_{O(^1D)}$ in different atmospheres (Stone et al., 2012), such an assumption seems to be reasonable. When isoprene is in a steady state in the atmosphere, OS_i production is expected to be proportional to the product of O_3, UV, and sulfate.

$$\frac{d[OS_i]}{dt} \propto UV[O_3][SO_4^{2-}] \quad (12)$$

It should be noted that equation (12) did not consider the influences of aerosol acidity, ALW, and other factors (e.g., •OH production from the photolysis of nitrous acid and aldehydes during the daytime). However, the deduction can at least suggest that the secondary production of OS_i is positively correlated with the value of $UV[O_3][SO_4^{2-}]$. Indeed, the concentrations of daytime OS_i and major OS_i species showed a linear positive relationship with the value of $UV[O_3][SO_4^{2-}]$ at both urban and suburban sites (r = 0.84–0.92, P < 0.01) (**Figure 4a-c**). We found that the correlation between major OS_i species and $UV[O_3][SO_4^{2-}]$ was stronger than the correlation of major OS_i species with O_3 and SO_4^{2-} (r < 0.82, P < 0.01); moreover, there was no significant correlation between major OSs and UV (P > 0.05). Thus, our results provide field evidence that the formation of daytime OS_i in these two study areas was mainly controlled by •OH oxidation of isoprene; moreover, the higher concentration of OS_i in the urban area can be attributed to the stronger atmospheric oxidation capacity (i.e., higher $UV[O_3]$ value) and more serious anthropogenic sulfate pollution (particularly during period A). We also observed that the OS concentrations did not significantly increase in several high sulfate events in the period B. One possible explanation is that

https://doi.org/10.5194/egusphere-2023-1292
Preprint. Discussion started: 14 June 2023

these abnormal high sulfate events resulted in excessive SO_4^{2-} in the formation of OSs.

2-MT-OS and 2-MGA-OS have been identified as important tracers of isoprene-derived SOA (Hettiyadura et al. 2019; Cai et al. 2020). During isoprene oxidation by •OH, these two OS species are produced under low (i.e., IEPOX pathway) and high (i.e., HMML or methacrylic acid epoxide (MAE) pathways) NO_x conditions, respectively (Surratt et al. 2010; Nguyen et al. 2015). The ratios of 2-MT-OS concentration to 2-MGA-OS concentration in the daytime were 9.7 ± 3.1 and 12.1 ± 5.5 at urban and suburban sites, respectively (**Figure S5b**). A 2-MT-OS/2-MGA-OS ratio of larger than 1 was also found in observations in summer 2020 (**Figure S5a**), suggesting low NO_x channel dominated the formation of daytime OS_i in the two study areas. This finding was similar to previous observations in Beijing (3.2) (Wang et al. 2020) and Guangzhou (7.6) (Bryant et al. 2021). Other abundant OS_i compounds including $C_5H_7O_7S^-$, $C_4H_7O_6S^-$, and $C_5H_9O_7S^-$ can be produced by the photooxidation of isoprene, heterogeneous oxidative aging of 2-MT-OS, or sulfate radical-initiated reaction with methacrolein and methyl vinyl ketone in the aqueous phase (Schindelka et al. 2013; Wach et al. 2019; Hettiyadura et al. 2015). These OSs showed strong correlations (r = 0.74–0.90, P < 0.01) with UV$[O_3][SO_4^{2-}]$, which further highlights the significance of the photochemistry in OS_i formation.

In the nighttime, the formation •OH can be primarily attributed to the reactions of olefins and O_3 (Paulson and Orlando 1996). As shown in **Figures 4d-f**, total OS_i and major OS_i compounds were significantly correlated with the product of O_3 and SO_4^{2-} concentrations (P < 0.01, r = 0.96–0.98). Since the nighttime oxidant level (including

https://doi.org/10.5194/egusphere-2023-1292
Preprint. Discussion started: 14 June 2023

O_3 and •OH) was substantially lower than that in the daytime (**Table S5**), the production of OS_i was weakened in the nighttime (**Table S2**). It is interesting to note the 2-MT-OS/2-MGA-OS mean ratio in the nighttime was 13.1–15.0 (**Figure S5(b)**), significantly higher than the mean ratio (9.7–12.1) in the daytime, indicating that the IEPOX pathway may be a potential mechanism to generate OS_i in the nighttime. Another possible explanation for the smaller OS concentration in the nighttime is that these OSs were mainly formed during the daytime, but had a significantly lower concentration in the nighttime due to the dilution and deposition.

Furthermore, NO_3• chemistry in the nighttime was another possible pathway to form OS_i, particularly NOSs. The nighttime NOS concentration was linearly correlated with the product of NO_2 and O_3 ($[NO_2][O_3]$, i.e., a proxy of NO_3•) (**Figure S6**). Interestingly, most of NOS_i (e.g., $C_5H_{10}NO_9S^-$, $C_5H_8NO_{10}S^-$, $C_4H_8NO_7S^-$, and $C_5H_8NO_7S^-$) have higher concentrations in the daytime, excepting for $C_5H_9N_2O_{11}S^-$. Thus, although nighttime NO_3• chemistry was important, the NOS_i formed via photochemistry under the influence of NO_x in the daytime was still dominant contributors to total NOS_i in our study areas. Regarding $C_5H_9N_2O_{11}S^-$, its formation pathway is mainly the NO_3• oxidation of $C_5H_9NO_5$ as illustrated in **Figure S7** (Hamilton et al. 2021). Accordingly, the abundance of $C_5H_9N_2O_{11}S^-$ peaked during the nighttime (**Figure S8**). It should be pointed out that the •OH oxidation of $C_5H_9NO_5$ can also contribute to the production of $C_5H_{10}NO_9S^-$ (**Figure S7**). Clearly, this mechanism can be responsible for the higher $C_5H_{10}NO_9S^-$ concentrations in the daytime as mentioned above. In general, increased OS_i level in the daytime demonstrated that the

https://doi.org/10.5194/egusphere-2023-1292
Preprint. Discussion started: 14 June 2023

formation of OS_i in urban and suburban areas was largely controlled by photooxidation of isoprene in the presence of sulfate in the daytime, rather than nighttime NO_3• chemistry. Moreover, a decrease in average OS_i level from the urban area to the suburban area can be explained by the weakened photooxidation of isoprene and the decreased anthropogenic sulfate pollution (particularly in the relatively polluted period).

3.3.2 Monoterpene-derived OSs

The concentrations of the most abundant OS_m species ($C_{10}H_{15}O_7S^-$ and $C_8H_{13}O_7S^-$) showed a strong correlation with the value of $UV[O_3][SO_4^{2-}]$ (and $UV[O_3][SO_2]$) in the daytime at both urban and suburban sites (r = 0.82–0.86, P < 0.01), indicating that the photooxidation of monoterpenes was a significant source for OS_m. Previous studies also demonstrated that $C_{10}H_{15}O_7S^-$ can be produced through the photooxidation of monoterpenes or sulfate radical reaction with α-pinene (Surratt et al. 2008; Nozière et al. 2010).

In the nighttime, the concentrations of nitrogen-free OS_m species decreased significantly with a decrease in the O_3 levels (Wang et al. 2020). However, NOS_m species increased in concentration in the nighttime and showed a significant correlation with the value of $[O_3][NO_2]$ (the proxy of NO_3•, as mentioned above) (r = 0.90–0.95, P < 0.01). Accordingly, nighttime NO_3• chemistry exerted a significant influence on the abundance of NOS_m in these study areas. A study by Hamilton et al., (2021) has reported that NO_3• chemistry plays an important role in the production of NOS_m. However, the overall lower OS_m level in the nighttime (**Table S2**) suggests that daytime OS_m

https://doi.org/10.5194/egusphere-2023-1292
Preprint. Discussion started: 14 June 2023

production via monoterpenes photooxidation was still the dominant contributor to total OS_m throughout the day. Although several filed studies have reported the abundance of various NOS_m (e.g., $C_{10}H_{16}NO_7S^-$ and $C_9H_{14}NO_8S^-$) (Wang et al. 2018; Bryant et al. 2021; Cai et al. 2020), their structures, formation mechanisms, and relevant diurnal variations remain large uncertainties, which need to be deeply explored in the future research.

3.3.3 C_2-C_3 and anthropogenic OSs

The OS species with two or three carbon atoms (C_2-C_3 OSs) are generally considered to originate from both biogenic and anthropogenic emissions (Wang et al. 2020). The abundant C_2-C_3 OS species, including $C_2H_3O_6S^-$ (glycolic acid sulfate; GAS), $C_3H_5O_5S^-$ (hydroxyacetone sulfate; HAS), and $C_3H_5O_6S^-$ (lactic acid sulfate; LAS), were significantly correlated with the values of $UV[O_3][SO_4^{2-}]$ in the daytime at both urban and suburban sites (r = 0.79–0.91, P < 0.01), indicating that the photochemical processes largely contributed to the formation of C_2-C_3 OSs. Recently, the heterogeneous •OH oxidation of particulate 2-MT-OS has been shown to generate a series of C_2-C_3 OSs (e.g., $C_2H_3O_6S^-$, $C_3H_5O_6S^-$, and $C_2H_3O_5S^-$) (Chen et al. 2020). Moreover, $C_3H_5O_4S^-$ and $C_3H_7O_5S^-$ have previously been reported to be produced by the photooxidation of diesel vehicle exhausts (Blair et al. 2017).

Most of the quantified OS_a compounds, including $C_{13}H_{25}O_5S^-$, $C_9H_{15}O_7S^-$, $C_8H_{17}O_4S^-$, benzyl sulfate ($C_7H_7O_4S^-$), phenyl sulfate ($C_6H_5O_4S^-$), as well as $C_6H_9O_6S^-$, $C_5H_7O_6S^-$, and $C_4H_7O_4S^-$, exhibited a strong correlation (P < 0.01) with the values of $UV[O_3][SO_4^{2-}]$ in the daytime. $C_{13}H_{25}O_5S^-$ has been detected in diesel exhaust

https://doi.org/10.5194/egusphere-2023-1292
Preprint. Discussion started: 14 June 2023

(Cui et al. 2019), which is the homologous compound of $C_{12}H_{23}O_5S^-$ produced from dodecane photooxidation (Riva et al. 2016b). A chamber study has detected $C_9H_{15}O_7S^-$ in decalin SOA and speculated that it was produced via •OH oxidation of a C_9-carbonyl hydroperoxide ($C_9H_{16}O_3$) and subsequent reaction on acidic sulfate aerosols (Riva et al. 2016b). In addition, photooxidation of diesel fuel vapor in the presence of SO_2 has been suggested to be an important source of $C_6H_9O_6S^-$, $C_5H_7O_6S^-$, and $C_4H_7O_4S^-$ species (Blair et al. 2017). The formation of $C_7H_7O_4S^-$ and $C_6H_5O_4S^-$ can also be attributed to the photooxidation of naphthalene and 2-methylnaphthalene (Riva et al. 2015).

We note that the concentrations of most of C_2-C_3 OS and OS_a species decreased significantly from the daytime to the nighttime (**Table S2** and **Table S3**). The dilution and deposition effects from the daytime to the nighttime were important factors controlling nighttime levels of C_2-C_3 OSs and OS_a. In addition, the nighttime gas-phase oxidation process was also likely associated with C_2-C_3 and anthropogenic OS formation at both urban and suburban sites, as suggested by the significant correlations of C_2-C_3 OSs and OS_a with O_3 and $[O_3][NO_2]$ in the nighttime ($r = 0.89$–0.91, $P < 0.01$). Overall, these results further highlight the importance of photochemistry in controlling the all-day abundance of OSs, as discussed earlier.

3.3.4 The effects of ALW and pH on OS formation

We have demonstrated that the atmospheric oxidation capacity (e.g., UV$[O_3]$ and $[O_3 + NO_2]$), sulfate pollution, and nighttime NO_3• chemistry exerted considerable influences on the formation of OSs in both urban and suburban areas. In addition,

https://doi.org/10.5194/egusphere-2023-1292
Preprint. Discussion started: 14 June 2023

laboratory and field studies have suggested that aerosol properties including acidity and ALW also play important roles in OS formation (Iinuma et al. 2007; Surratt et al. 2007b; Wang et al. 2020; Wang et al. 2018; 2022). The aerosol pH in Shanghai in summer averaged 2.7 ± 0.9 and 2.2 ± 0.7 in urban and suburban areas, respectively. The mean pH value was similar to that in northern China (summer) (Ding et al. 2019; Wang et al. 2018), but higher than that in the Pearl River Delta (PRD) region (Fu et al. 2015). In this study, only the 2-MT-OS concentration showed an evident negative correlation with the pH value ($r = 0.58$, $P < 0.05$), suggesting the aerosol acidity is not a limiting factor for the formation of most OS species.

A positive correlation was observed between the concentrations of OSs and ALW only in the urban area during both daytime and nighttime (**Figure 5**), consistent with our previous observations in urban Shanghai (Wang et al. 2021). It is interesting to note that although higher ALW concentrations and lower pH values were observed at the suburban site, the OS concentrations were significantly higher at the urban site (**Table S5**). This result further confirms that atmospheric oxidation capacity and sulfate pollution level governed the formation of OSs in urban and suburban Shanghai (particularly in the relatively polluted period), though ALW and aerosol acidity also played a role. Therefore, a synergistic regulation of atmospheric oxidation capacity and anthropogenic SO_2 emissions would be important for the mitigation of OS and SOA pollution in the megacity Shanghai.

4. Conclusions

https://doi.org/10.5194/egusphere-2023-1292
Preprint. Discussion started: 14 June 2023

We investigated the spatial and diurnal variations of aerosol OS formation in Shanghai in summer. Isoprene- and monoterpene-derived OSs were found to be the dominant OS groups during the entire sampling campaign, likely suggesting that the formation of OSs was largely controlled by biogenic VOCs. Most OSs decreased from the daytime to the nighttime, while NOS_m peaked during nighttime. These findings suggested that OSs were mainly produced via daytime formation processes in both urban and suburban areas, excepting NOS_m. Moreover, the average abundance of various types of OSs showed a decrease trend from the urban area to the suburban area, which can be explained by weakened atmospheric oxidation capacity and sulfate pollution in the suburban area (primarily in the relatively polluted period). Further, daytime OS formation was concretized according to the interactions among OSs, UV, O_3, and SO_4^{2-}, suggesting that the concentrations of most OSs were significantly correlated with the values of UV$[O_3][SO_4^{2-}]$ during daytime in both urban and suburban Shanghai. We concluded that an enhancement in the photochemical process and sulfate level can exacerbate OS pollution in the urban area. These findings were summarized in a diagram (**Figure 6**). Generally, our study not only deepens the understanding about the importance of photochemical process and anthropogenic sulfate pollution in controlling OS formation but also provides potential management strategies to decrease the abundance of particulate OSs.

Data availability

The data presented in this work are available upon request from the corresponding

https://doi.org/10.5194/egusphere-2023-1292
Preprint. Discussion started: 14 June 2023

authors.

Supplement

Supplementary information includes the classification of OSs, Table S1-S5, and Figure S1−S8.

Competing interests

The authors declare no competing financial interest.

Disclaimer

Publisher's note: Copernicus Publications remains neutral with regard to jurisdictional claims in published maps and institutional affiliations.

Acknowledgements

This study was supported by the National Natural Science Foundation of China (grant 22022607), the Program for Professor of Special Appointment (Eastern Scholar) at Shanghai Institutions of Higher Learning, the Shanghai Sailing Program (grant 22YF1418700), the Shanghai Pujiang Program (grant 20PJ1407600), and the National Natural Science Foundation of China (grant 42005090).

https://doi.org/10.5194/egusphere-2023-1292
Preprint. Discussion started: 14 June 2023

References

Berndt, T., Richters, S., Jokinen, T., Hyttinen, N., Kurten, T., Otkjaer, R. V., Kjaergaard, H. G., Stratmann, F., Herrmann, H., Sipila, M., Kulmala, M., and Ehn, M.: Hydroxyl radical-induced formation of highly oxidized organic compounds, Nat. Commun., 7, 13677, 10.1038/ncomms13677, 2016.

Blair, S. L., MacMillan, A. C., Drozd, G. T., Goldstein, A. H., Chu, R. K., Pasa-Tolic, L., Shaw, J. B., Tolic, N., Lin, P., Laskin, J., Laskin, A., and Nizkorodov, S. A.: Molecular Characterization of Organosulfur Compounds in Biodiesel and Diesel Fuel Secondary Organic Aerosol, Environ. Sci. Technol., 51, 119-127, 10.1021/acs.est.6b03304, 2017.

Bryant, D. J., Elzein, A., Newland, M., White, E., Swift, S., Watkins, A., Deng, W., Song, W., Wang, S., Zhang, Y., Wang, X., Rickard, A. R., and Hamilton, J. F.: Importance of Oxidants and Temperature in the Formation of Biogenic Organosulfates and Nitrooxy Organosulfates, ACS Earth Space Chem., 5, 2291-2306, 10.1021/acsearthspacechem.1c00204, 2021.

Cai, D., Wang, X., Chen, J., and Li, X.: Molecular Characterization of Organosulfates in Highly Polluted Atmosphere Using Ultra-High-Resolution Mass Spectrometry, J. Geophys. Res.: Atmos. , 125, 10.1029/2019jd032253, 2020.

Chen, Y., Zhang, Y., Lambe, A. T., Xu, R., Lei, Z., Olson, N. E., Zhang, Z., Szalkowski, T., Cui, T., Vizuete, W., Gold, A., Turpin, B. J., Ault, A. P., Chan, M. N., and Surratt,

https://doi.org/10.5194/egusphere-2023-1292
Preprint. Discussion started: 14 June 2023

575 J. D.: Heterogeneous Hydroxyl Radical Oxidation of Isoprene-Epoxydiol-Derived
576 Methyltetrol Sulfates: Plausible Formation Mechanisms of Previously
577 Unexplained Organosulfates in Ambient Fine Aerosols, Environ. Sci.
578 Technol.Lett., 7, 460-468, 10.1021/acs.estlett.0c00276, 2020.
579 Cui, M., Li, C., Chen, Y., Zhang, F., Li, J., Jiang, B., Mo, Y., Li, J., Yan, C., Zheng, M.,
580 Xie, Z., Zhang, G., and Zheng, J.: Molecular characterization of polar organic
581 aerosol constituents in off-road engine emissions using Fourier transform ion
582 cyclotron resonance mass spectrometry (FT-ICR MS): implications for source
583 apportionment, Atmos. Chem. Phys., 19, 13945-13956, 10.5194/acp-19-13945-
584 2019, 2019.
585 Ding, J., Zhao, P., Su, J., Dong, Q., Du, X., and Zhang, Y.: Aerosol pH and its driving
586 factors in Beijing, Atmos. Chem. Phys., 19, 7939-7954, 10.5194/acp-19-7939-
587 2019, 2019.
588 Estillore, A. D., Hettiyadura, A. P., Qin, Z., Leckrone, E., Wombacher, B., Humphry, T.,
589 Stone, E. A., and Grassian, V. H.: Water Uptake and Hygroscopic Growth of
590 Organosulfate Aerosol, Environ Sci Technol, 50, 4259-4268,
591 10.1021/acs.est.5b05014, 2016.
592 Fabien, P., John, D. C., Henrik, G. K., Andreas, k., Jason, M. S. C., John, H. S., and
593 Paul, O. W.: Unexpected Epoxide Formation in the Gas-Phase Photooxidation of
594 Isoprene, Science, 325, 730-733, 2009.
595 Fleming, L. T., Ali, N. N., Blair, S. L., Roveretto, M., George, C., and Nizkorodov, S.
596 A.: Formation of Light-Absorbing Organosulfates during Evaporation of

https://doi.org/10.5194/egusphere-2023-1292
Preprint. Discussion started: 14 June 2023

Secondary Organic Material Extracts in the Presence of Sulfuric Acid, ACS Earth Space Chem., 3, 947-957, 10.1021/acsearthspacechem.9b00036, 2019.

Fu, X., Guo, H., Wang, X., Ding, X., He, Q., Liu, T., and Zhang, Z.: PM2.5 acidity at a background site in the Pearl River Delta region in fall-winter of 2007-2012, J. Hazard. Mater., 286, 484-492, 10.1016/j.jhazmat.2015.01.022, 2015.

Gani, S., Bhandari, S., Seraj, S., Wang, D. S., Patel, K., Soni, P., Arub, Z., Habib, G., Hildebrandt Ruiz, L., and Apte, J. S.: Submicron aerosol composition in the world's most polluted megacity: the Delhi Aerosol Supersite study, Atmos. Chem. Phys., 19, 6843-6859, 10.5194/acp-19-6843-2019, 2019.

Glasius, M., Thomsen, D., Wang, K., Iversen, L. S., Duan, J., and Huang, R. J.: Chemical characteristics and sources of organosulfates, organosulfonates, and carboxylic acids in aerosols in urban Xi'an, Northwest China, Sci Total Environ, 810, 151187, 10.1016/j.scitotenv.2021.151187, 2022.

Guo, H., Xu, L., Bougiatioti, A., Cerully, K. M., Capps, S. L., Hite Jr, J. R., Carlton, A. G., Lee, S. H., Bergin, M. H., Ng, N. L., Nenes, A., and Weber, R. J.: Fine-particle water and pH in the southeastern United States, Atmos. Chem. Phys., 15, 5211-5228, 10.5194/acp-15-5211-2015, 2015.

H., J. and Seinfeld, S. N. P.: Atmospheric chemistry and physics: from air pollution to climate change, 2016.

Hamilton, J. F., Bryant, D. J., Edwards, P. M., Ouyang, B., Bannan, T. J., Mehra, A., Mayhew, A. W., Hopkins, J. R., Dunmore, R. E., Squires, F. A., Lee, J. D., Newland, M. J., Worrall, S. D., Bacak, A., Coe, H., Percival, C., Whalley, L. K.,

https://doi.org/10.5194/egusphere-2023-1292
Preprint. Discussion started: 14 June 2023

Heard, D. E., Slater, E. J., Jones, R. L., Cui, T., Surratt, J. D., Reeves, C. E., Mills, G. P., Grimmond, S., Sun, Y., Xu, W., Shi, Z., and Rickard, A. R.: Key Role of NO3 Radicals in the Production of Isoprene Nitrates and Nitrooxyorganosulfates in Beijing, Environ. Sci. Technol., 55, 842-853, 10.1021/acs.est.0c05689, 2021.

Hawkins, L. N., Russell, L. M., Covert, D. S., Quinn, P. K., and Bates, T. S.: Carboxylic acids, sulfates, and organosulfates in processed continental organic aerosol over the southeast Pacific Ocean during VOCALS-REx 2008, J. Geophys. Res.: Atmos. , 115, 10.1029/2009jd013276, 2010.

Hennigan, C. J., Izumi, J., Sullivan, A. P., Weber, R. J., and Nenes, A.: A critical evaluation of proxy methods used to estimate the acidity of atmospheric particles, Atmos. Chem. Phys., 15, 2775-2790, 10.5194/acp-15-2775-2015, 2015.

Hettiyadura, A. P. S., Al-Naiema, I. M., Hughes, D. D., Fang, T., and Stone, E. A.: Organosulfates in Atlanta, Georgia: anthropogenic influences on biogenic secondary organic aerosol formation, Atmos. Chem. Phys., 19, 3191-3206, 10.5194/acp-19-3191-2019, 2019.

Hettiyadura, A. P. S., Stone, E. A., Kundu, S., Baker, Z., Geddes, E., Richards, K., and Humphry, T.: Determination of atmospheric organosulfates using HILIC chromatography with MS detection, Atoms. Meas. Tech., 8, 2347-2358, 10.5194/amt-8-2347-2015, 2015.

Hettiyadura, A. P. S., Jayarathne, T., Baumann, K., Goldstein, A. H., de Gouw, J. A., Koss, A., Keutsch, F. N., Skog, K., and Stone, E. A.: Qualitative and quantitative analysis of atmospheric organosulfates in Centreville, Alabama, Atmos. Chem.

https://doi.org/10.5194/egusphere-2023-1292
Preprint. Discussion started: 14 June 2023

Phys., 17, 1343-1359, 10.5194/acp-17-1343-2017, 2017.

Hughes, D. D., Christiansen, M. B., Milani, A., Vermeuel, M. P., Novak, G. A., Alwe, H. D., Dickens, A. F., Pierce, R. B., Millet, D. B., Bertram, T. H., Stanier, C. O., and Stone, E. A.: PM2.5 chemistry, organosulfates, and secondary organic aerosol during the 2017 Lake Michigan Ozone Study, Atmos. Environ., 244, 10.1016/j.atmosenv.2020.117939, 2021.

Iinuma , Müller , Berndt , Böge , Claeys， , and Herrmann: Evidence for the Existence of Organosulfates from β-Pinene Ozonolysis in Ambient Secondary Organic Aerosol, Environ. Sci. Technol., 41, 6678-6683, 2007.

Iinuma, Y., Müller, C., Böge, O., Gnauk, T., and Herrmann, H.: The formation of organic sulfate esters in the limonene ozonolysis secondary organic aerosol (SOA) under acidic conditions, Atmos. Environ., 41, 5571-5583, 10.1016/j.atmosenv.2007.03.007, 2007.

Kanellopoulos, P. G., Kotsaki, S. P., Chrysochou, E., Koukoulakis, K., Zacharopoulos, N., Philippopoulos, A., and Bakeas, E.: PM2.5-bound organosulfates in two Eastern Mediterranean cities: The dominance of isoprene organosulfates, Chemosphere, 297, 134103, 10.1016/j.chemosphere.2022.134103, 2022.

Kourtchev, I., Doussin, J. F., Giorio, C., Mahon, B., Wilson, E. M., Maurin, N., Pangui, E., Venables, D. S., Wenger, J. C., and Kalberer, M.: Molecular composition of fresh and aged secondary organic aerosol from a mixture of biogenic volatile compounds: a high-resolution mass spectrometry study, Atmos. Chem. Phys., 15, 5683-5695, 10.5194/acp-15-5683-2015, 2015.

https://doi.org/10.5194/egusphere-2023-1292
Preprint. Discussion started: 14 June 2023

663 Kristensen, K. and Glasius, M.: Organosulfates and oxidation products from biogenic
664 hydrocarbons in fine aerosols from a forest in North West Europe during spring,
665 Atmos. Environ., 45, 4546-4556, 10.1016/j.atmosenv.2011.05.063, 2011.
666 Li, X., Zhang, Y., Shi, L., Kawamura, K., Kunwar, B., Takami, A., Arakaki, T., and Lai,
667 S.: Aerosol Proteinaceous Matter in Coastal Okinawa, Japan: Influence of Long-
668 Range Transport and Photochemical Degradation, Environ Sci Technol, 56, 5256-
669 5265, 10.1021/acs.est.1c08658, 2022.
670 Lin, Y., Han, Y., Li, G., Wang, Q., Zhang, X., Li, Z., Li, L., Prévôt, A. S. H., and Cao,
671 J.: Molecular Characteristics of Atmospheric Organosulfates During Summer and
672 Winter Seasons in Two Cities of Southern and Northern China, J. Geophys. Res.:
673 Atmos. , 127, 10.1029/2022jd036672, 2022.
674 Menon, S., ;, Unger, N., ;, Koch, D., ;, Francis, J., ;, Garrett, T., ;, Sednev, I., ;, Shindell,
675 D., ;, and Streets, D., ;: Aerosol climate effects and air quality impacts from 1980
676 to 2030, Environ. Res. Lett., 3, 10.1088/1748-9326/3/2/024004, 2008.
677 Nestorowicz, K., Jaoui, M., Rudzinski, K. J., Lewandowski, M., Kleindienst, T. E.,
678 Spolnik, G., Danikiewicz, W., and Szmigielski, R.: Chemical composition of
679 isoprene SOA under acidic and non-acidic conditions: effect of relative humidity,
680 Atmos Chem Phys, 18, 18101-18121, 10.5194/acp-18-18101-2018, 2018.
681 Nguyen, Q. T., Christensen, M. K., Cozzi, F., Zare, A., Hansen, A. M. K., Kristensen,
682 K., Tulinius, T. E., Madsen, H. H., Christensen, J. H., Brandt, J., Massling, A.,
683 Nøjgaard, J. K., and Glasius, M.: Understanding the anthropogenic influence on
684 formation of biogenic secondary organic aerosols in Denmark via analysis of

https://doi.org/10.5194/egusphere-2023-1292
Preprint. Discussion started: 14 June 2023

organosulfates and related oxidation products, Atmos. Chem. Phys., 14, 8961-8981, 10.5194/acp-14-8961-2014, 2014.

Nguyen, T. B., Bates, K. H., Crounse, J. D., Schwantes, R. H., Zhang, X., Kjaergaard, H. G., Surratt, J. D., Lin, P., Laskin, A., Seinfeld, J. H., and Wennberg, P. O.: Mechanism of the hydroxyl radical oxidation of methacryloyl peroxynitrate (MPAN) and its pathway toward secondary organic aerosol formation in the atmosphere, Phys. Chem. Chem. Phys., 17, 17914-17926, 10.1039/c5cp02001h, 2015.

Nozière, B., Ekström, S., Alsberg, T., and Holmström, S.: Radical-initiated formation of organosulfates and surfactants in atmospheric aerosols, Geophys. Res. Lett., 37, n/a-n/a, 10.1029/2009gl041683, 2010.

Olson, C. N., Galloway, M. M., Yu, G., Hedman, C. J., Lockett, M. R., Yoon, T., Stone, E. A., Smith, L. M., and Keutsch, F. N.: Hydroxycarboxylic acid-derived organosulfates: synthesis, stability, and quantification in ambient aerosol, Environ Sci Technol, 45, 6468-6474, 10.1021/es201039p, 2011.

Passananti, M., Kong, L., Shang, J., Dupart, Y., Perrier, S., Chen, J., Donaldson, D. J., and George, C.: Organosulfate Formation through the Heterogeneous Reaction of Sulfur Dioxide with Unsaturated Fatty Acids and Long-Chain Alkenes, Angew. Chem. Int. Ed. Engl., 55, 10336-10339, 10.1002/anie.201605266, 2016.

Paulson, S. E. and Orlando, J. J.: The reactions of ozone with alkenes: An important source of HOxin the boundary layer, Geophys. Res. Lett., 23, 3727-3730, 10.1029/96gl03477, 1996.

https://doi.org/10.5194/egusphere-2023-1292
Preprint. Discussion started: 14 June 2023

Ramanathan , V., Crutzen, P. J., Kiehl, J. T., and Rosenfeld, D.: Aerosols, Climate, and the Hydrological Cycle, Science, 294, 2119-2124, 2001.

Riva, M., Budisulistiorini, S. H., Zhang, Z., Gold, A., and Surratt, J. D.: Chemical characterization of secondary organic aerosol constituents from isoprene ozonolysis in the presence of acidic aerosol, Atmospheric Environment, 130, 5-13, 10.1016/j.atmosenv.2015.06.027, 2016a.

Riva, M., Da Silva Barbosa, T., Lin, Y.-H., Stone, E. A., Gold, A., and Surratt, J. D.: Chemical characterization of organosulfates in secondary organic aerosol derived from the photooxidation of alkanes, Atmos. Chem. Phys., 16, 11001-11018, 10.5194/acp-16-11001-2016, 2016b.

Riva, M., Tomaz, S., Cui, T., Lin, Y. H., Perraudin, E., Gold, A., Stone, E. A., Villenave, E., and Surratt, J. D.: Evidence for an unrecognized secondary anthropogenic source of organosulfates and sulfonates: gas-phase oxidation of polycyclic aromatic hydrocarbons in the presence of sulfate aerosol, Environ. Sci. Technol., 49, 6654-6664, 10.1021/acs.est.5b00836, 2015.

Riva, M., Chen, Y., Zhang, Y., Lei, Z., Olson, N. E., Boyer, H. C., Narayan, S., Yee, L. D., Green, H. S., Cui, T., Zhang, Z., Baumann, K., Fort, M., Edgerton, E., Budisulistiorini, S. H., Rose, C. A., Ribeiro, I. O., RL, E. O., Dos Santos, E. O., Machado, C. M. D., Szopa, S., Zhao, Y., Alves, E. G., de Sa, S. S., Hu, W., Knipping, E. M., Shaw, S. L., Duvoisin Junior, S., de Souza, R. A. F., Palm, B. B., Jimenez, J. L., Glasius, M., Goldstein, A. H., Pye, H. O. T., Gold, A., Turpin, B. J., Vizuete, W., Martin, S. T., Thornton, J. A., Dutcher, C. S., Ault, A. P., and Surratt,

https://doi.org/10.5194/egusphere-2023-1292
Preprint. Discussion started: 14 June 2023

J. D.: Increasing Isoprene Epoxydiol-to-Inorganic Sulfate Aerosol Ratio Results in Extensive Conversion of Inorganic Sulfate to Organosulfur Forms: Implications for Aerosol Physicochemical Properties, Environ. Sci. Technol., 53, 8682-8694, 10.1021/acs.est.9b01019, 2019.

Schindelka, J., Iinuma, Y., Hoffmann, D., and Herrmann, H.: Sulfate radical-initiated formation of isoprene-derived organosulfates in atmospheric aerosols, Faraday Discuss., 165, 237-259, 10.1039/c3fd00042g, 2013.

Shalamzari, M. S., Ryabtsova, O., Kahnt, A., Vermeylen, R., Herent, M. F., Quetin-Leclercq, J., Van der Veken, P., Maenhaut, W., and Claeys, M: Mass spectrometric characterization of organosulfates related to secondary organic aerosol from isoprene, Rapid Commun. Mass Spectrom., 784-794, 10.1002/rcm.6511, 2013, 2013.

Shang, J., Passananti, M., Dupart, Y., Ciuraru, R., Tinel, L., Rossignol, S., Perrier, S., Zhu, T., and George, C.: SO2 Uptake on Oleic Acid: A New Formation Pathway of Organosulfur Compounds in the Atmosphere, Environ. Sci. Technol.Lett., 3, 67-72, 10.1021/acs.estlett.6b00006, 2016.

Seinfeld, J. H., Pandis, S., N.,: Atmospheric chemistry and physics: from air pollution to climate change, 2016.

Stone, E. A., Yang, L., Yu, L. E., and Rupakheti, M.: Characterization of organosulfates in atmospheric aerosols at Four Asian locations, Atmos. Environ., 47, 323-329, 10.1016/j.atmosenv.2011.10.058, 2012.

Surratt, J. D., Lewandowski, M., Offenberg, J. H., Jaoui, M., Kleindienst, T.E., Edney,

https://doi.org/10.5194/egusphere-2023-1292
Preprint. Discussion started: 14 June 2023

E. O., and Seinfeld, J. H.: Effect of Acidity on Secondary Organic Aerosol Formation from Isoprene, Environ. Sci. Technol., 41, 5363–5369, 2007a.

Surratt, J. D., Chan, A. W., Eddingsaas, N. C., Chan, M., Loza, C. L., Kwan, A. J., Hersey, S. P., Flagan, R. C., Wennberg, P. O., and Seinfeld, J. H.: Reactive intermediates revealed in secondary organic aerosol formation from isoprene, Proc. Natl. Acad. Sci. U.S.A., 107, 6640-6645, 10.1073/pnas.0911114107, 2010.

Surratt, J. D., Kroll, J. H., Kleindienst, T. E., Edney, E. O., Claeys, M., Sorooshian, A., Ng, N. L., Offenberg, J. H., Lewandowski, M., Jaoui, M., Flagan, R. C., and Seinfeld, J. H.: Evidence for Organosulfates in Secondary Organic Aerosol, Environ. Sci. Technol., 41, 517–527, 2007b.

Surratt, J. D., Gómez-González, Y., Chan, A. W. H., Vermeylen, R., Shahgholi, M., Kleindienst, T. E., Edney, E. O., Offenberg, J. H., Lewandowski, M., Jaoui, M., Maenhaut, W., Claeys, M., Flagan, R. C., and Seinfeld, J. H.: Organosulfate Formation in Biogenic Secondary Organic Aerosol, J. Phys. Chem. A., 112, 8345-8378, 10.1021/jp802310p, 2008.

Tao, S., Lu, X., Levac, N., Bateman, A. P., Nguyen, T. B., Bones, D. L., Nizkorodov, S. A., Laskin, J., Laskin, A., and Yang, X.: Molecular characterization of organosulfates in organic aerosols from Shanghai and Los Angeles urban areas by nanospray-desorption electrospray ionization high-resolution mass spectrometry, Environ. Sci. Technol., 48, 10993-11001, 10.1021/es5024674, 2014.

Tolocka, M. P. and Turpin, B.: Contribution of organosulfur compounds to organic aerosol mass, Environ. Sci. Technol., 46, 7978-7983, 10.1021/es300651v, 2012.

https://doi.org/10.5194/egusphere-2023-1292
Preprint. Discussion started: 14 June 2023

773 Turpin, B. J. and Lim, H.-J.: Species Contributions to PM2.5 Mass Concentrations:
774 Revisiting Common Assumptions for Estimating Organic Mass, Aerosol
775 Sci.Technol., 35, 602-610, 10.1080/02786820119445, 2001.
776 Vandergrift, G. W., Shawon, A. S. M., Dexheimer, D. N., Zawadowicz, M. A., Mei, F.,
777 and China, S.: Molecular Characterization of Organosulfate-Dominated Aerosols
778 over Agricultural Fields from the Southern Great Plains by High-Resolution Mass
779 Spectrometry, ACS Earth Space Chem., 10.1021/acsearthspacechem.2c00043,
780 2022.
781 Wach, P., Spolnik, G., Rudzinski, K. J., Skotak, K., Claeys, M., Danikiewicz, W., and
782 Szmigielski, R.: Radical oxidation of methyl vinyl ketone and methacrolein in
783 aqueous droplets: Characterization of organosulfates and atmospheric
784 implications, Chemosphere, 214, 1-9, 10.1016/j.chemosphere.2018.09.026, 2019.
785 Wang, Y., Ren, J., Huang, X. H. H., Tong, R., and Yu, J. Z.: Synthesis of Four
786 Monoterpene-Derived Organosulfates and Their Quantification in Atmospheric
787 Aerosol Samples, Environ. Sci. Technol., 51, 6791-6801, 10.1021/acs.est.7b01179,
788 2017.
789 Wang, Y., Ma, Y., Kuang, B., Lin, P., Liang, Y., Huang, C., and Yu, J. Z.: Abundance of
790 organosulfates derived from biogenic volatile organic compounds: Seasonal and
791 spatial contrasts at four sites in China, Sci. Total. Environ., 806, 151275,
792 10.1016/j.scitotenv.2021.151275, 2022.
793 Wang, Y., Zhao, Y., Wang, Y., Yu, J. Z., Shao, J., Liu, P., Zhu, W., Cheng, Z., Li, Z., Yan,
794 N., and Xiao, H.: Organosulfates in atmospheric aerosols in Shanghai, China:

https://doi.org/10.5194/egusphere-2023-1292
Preprint. Discussion started: 14 June 2023

seasonal and interannual variability, origin, and formation mechanisms, Atmos. Chem. Phys., 21, 2959-2980, 10.5194/acp-21-2959-2021, 2021.

Wang, Y., Hu, M., Wang, Y.-C., Li, X., Fang, X., Tang, R., Lu, S., Wu, Y., Guo, S., Wu, Z., Hallquist, M., and Yu, J. Z.: Comparative Study of Particulate Organosulfates in Contrasting Atmospheric Environments: Field Evidence for the Significant Influence of Anthropogenic Sulfate and NOx, Environ. Sci. Technol.Lett., 7, 787-794, 10.1021/acs.estlett.0c00550, 2020.

Wang, Y., Hu, M., Guo, S., Wang, Y., Zheng, J., Yang, Y., Zhu, W., Tang, R., Li, X., Liu, Y., Le Breton, M., Du, Z., Shang, D., Wu, Y., Wu, Z., Song, Y., Lou, S., Hallquist, M., and Yu, J.: The secondary formation of organosulfates under interactions between biogenic emissions and anthropogenic pollutants in summer in Beijing, Atmos. Chem. Phys., 18, 10693-10713, 10.5194/acp-18-10693-2018, 2018.

Xu, Y., Miyazaki, Y., Tachibana, E., Sato, K., Ramasamy, S., Mochizuki, T., Sadanaga, Y., Nakashima, Y., Sakamoto, Y., Matsuda, K., and Kajii, Y.: Aerosol Liquid Water Promotes the Formation of Water-Soluble Organic Nitrogen in Submicrometer Aerosols in a Suburban Forest, Environ. Sci. Technol., 54, 1406-1414, 10.1021/acs.est.9b05849, 2020.

Yassine, M. M., Dabek-Zlotorzynska, E., Harir, M., and Schmitt-Kopplin, P.: Identification of weak and strong organic acids in atmospheric aerosols by capillary electrophoresis/mass spectrometry and ultra-high-resolution Fourier transform ion cyclotron resonance mass spectrometry, Anal. Chem., 84, 6586-6594, 10.1021/ac300798g, 2012.

https://doi.org/10.5194/egusphere-2023-1292
Preprint. Discussion started: 14 June 2023

817 Ye, J., Abbatt, J. P. D., and Chan, A. W. H.: Novel pathway of SO2 oxidation in the
818 atmosphere:reactions with monoterpene ozonolysis intermediates and secondary
819 organic aerosol, Atmos. Chem. Phys., 18, 5549-5565, 10.5194/acp-18-5549-2018,
820 2018.
821 Ye, Y., Zhan, H., Yu, X., Li, J., Wang, X., and Xie, Z.: Detection of organosulfates and
822 nitrooxy-organosulfates in Arctic and Antarctic atmospheric aerosols, using ultra-
823 high resolution FT-ICR mass spectrometry, Sci. Total. Environ., 767, 144339,
824 10.1016/j.scitotenv.2020.144339, 2021.

825
826
827
828
829
830

https://doi.org/10.5194/egusphere-2023-1292
Preprint. Discussion started: 14 June 2023

831 **Table S1.** Organosulfate quantification using UPLC-ESI(-)-QToFMS(/MS).

Formula[a]	MW (Da)	Standard	Reference
Isoprene-derived OSs (*n* = 19)			
$C_4H_7O_5S^-$	167.0014	Lactic acid sulfate (LAS)	(Schindelka et al. 2013)
$C_4H_7O_6S^-$	182.9963	LAS	(Shalamzari 2013)
$C_5H_9O_6S^-$	197.0120	LAS	(Riva et al. 2016a)
$C_4H_7O_7S^-$	198.9912	LAS	(Hettiyadura et al. 2015)
$C_5H_{11}O_6S^-$	199.0276	LAS	(Riva et al. 2016a)
$C_5H_7O_7S^-$	210.9912	LAS	(Hettiyadura et al. 2015)
$C_5H_9O_7S^-$	213.0069	LAS	(Riva et al. 2016a)
$C_5H_{11}O_7S^-$	215.0225	LAS	(Surratt et al. 2010)
$C_7H_9O_7S^-$	237.0069	LAS	(Nozière et al. 2010)
$C_5H_{10}NO_9S^-$	260.0076	LAS	(Surratt et al. 2007a)
$C_5H_8NO_{10}S^-$	273.9869	LAS	(Nestorowicz et al. 2018)
Other quantified isoprene-derived OSs were shown in **SI**			
Monoterpene-derived OSs (*n* = 17)			
$C_7H_{11}O_6S^-$	223.0276	Glycolic acid sulfate (GAS)	(Yassine et al. 2012)
$C_7H_{11}O_7S^-$	239.0225	GAS	(Nozière et al. 2010)
$C_{10}H_{17}O_5S^-$	249.0797	α-Pinene sulfate	(Wang et al. 2017)
$C_8H_{13}O_7S^-$	253.0382	GAS	(Schindelka et al. 2013)
$C_{10}H_{15}O_7S^-$	279.0538	GAS	(Surratt et al. 2007a)
$C_{10}H_{17}O_7S^-$	281.0695	α-Pinene sulfate	(Nozière et al. 2010)
$C_{10}H_{16}NO_7S^-$	294.0647	α-Pinene sulfate	(Surratt et al. 2008)
$C_9H_{14}NO_8S^-$	296.0440	Limonaketone sulfate	(Surratt et al. 2008)
$C_{10}H_{16}NO_{10}S^-$	342.0495	Limonaketone sulfate	(Yassine et al. 2012)
$C_9H_{15}O_6S^-$	251.0589	Limonaketone sulfate	(Wang et al. 2017)
Other quantified monoterpene-derived OSs were shown in **SI**			
C_2-C_3 OSs (*n* = 6)			
$C_3H_5O_4S^-$	136.9909	GAS	(Yassine et al. 2012)
$C_2H_3O_5S^-$	138.9701	GAS	(Yassine et al. 2012)
$C_3H_5O_5S^-$	152.9858	GAS	(Hettiyadura et al. 2015)
$C_2H_3O_6S^-$	154.9650	GAS	(Olson et al. 2011)
$C_3H_7O_5S^-$	155.0014	GAS	(Hettiyadura et al. 2019)
$C_3H_5O_6S^-$	168.9807	LAS	(Olson et al. 2011)
OSa (aliphatic-OSs) (*n* = 53)			
$C_8H_{17}O_4S^-$	210.0926	Sodium octyl	(Wang et al. 2021)
Other quantified aliphatic-derived OSs were shown in **SI**			
OSa (aromatic-OSs) (*n* = 32)			
$C_6H_5O_4S^-$	172.9909	Methyl sulfate	(Wang et al. 2021)
$C_7H_7SO_4S^-$	218.9786	Methyl sulfate	(Wang et al. 2021)
Other quantified aromatic-derived OSs were shown in **SI**			
OS_a-other (*n* =3)			
$C_4H_7O_4S^-$	151.0065	Methyl sulfate	(Wang et al. 2021)
$C_5H_7O_6S^-$	194.9963	GAS	(Wang et al. 2021)
$C_6H_9O_6S^-$	209.0120	GAS	(Berndt et al. 2016)

832 [a] These compounds have been confirmed through structural identification with MS/MS.

https://doi.org/10.5194/egusphere-2023-1292
Preprint. Discussion started: 14 June 2023

833 **Figure 1.**

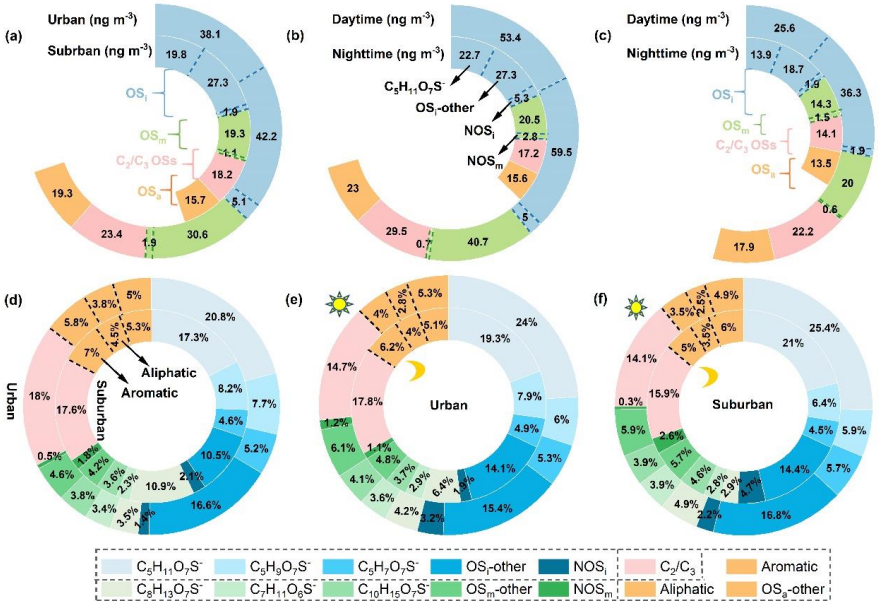

834

835 **Figure 1.** Average distributions in the mass concentrations and mass fractions of
836 various OSs in $PM_{2.5}$ in different cases: (a–d) urban vs suburban for all the data, (b–e)
837 daytime vs nighttime in the urban area, as well as (c–f) daytime vs nighttime in the
838 suburban area.

839
840

https://doi.org/10.5194/egusphere-2023-1292
Preprint. Discussion started: 14 June 2023

841 **Figure 2.**

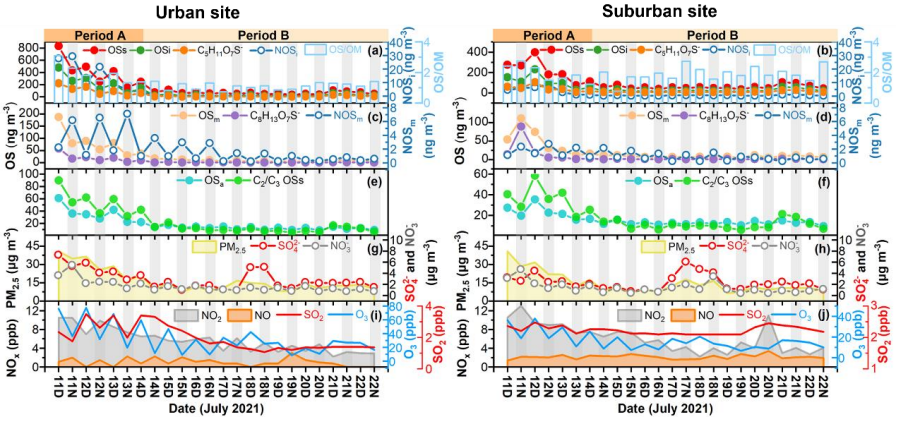

842

843 **Figure 2.** Temporal variations of OSs and other chemical components in $PM_{2.5}$ as well

844 as other data measured in urban and suburban Shanghai in summer. (a–b) OSs, OS_i,

845 $C_5H_{11}O_7S^-$, NOS_i, and OS/OM; (c–d) OS_m, $C_8H_{13}O_7S^-$, and NOS_m; (e–f) OS_a and C_2-

846 C_3 OSs; (g–h) $PM_{2.5}$, SO_4^{2-}, and NO_3^-; and (i–j) NO_2, NO, SO_2, and O_3. The sampling

847 period A and B indicate the relatively polluted period and the clean period, respectively.

848

https://doi.org/10.5194/egusphere-2023-1292
Preprint. Discussion started: 14 June 2023

849 **Figure 3.**

850

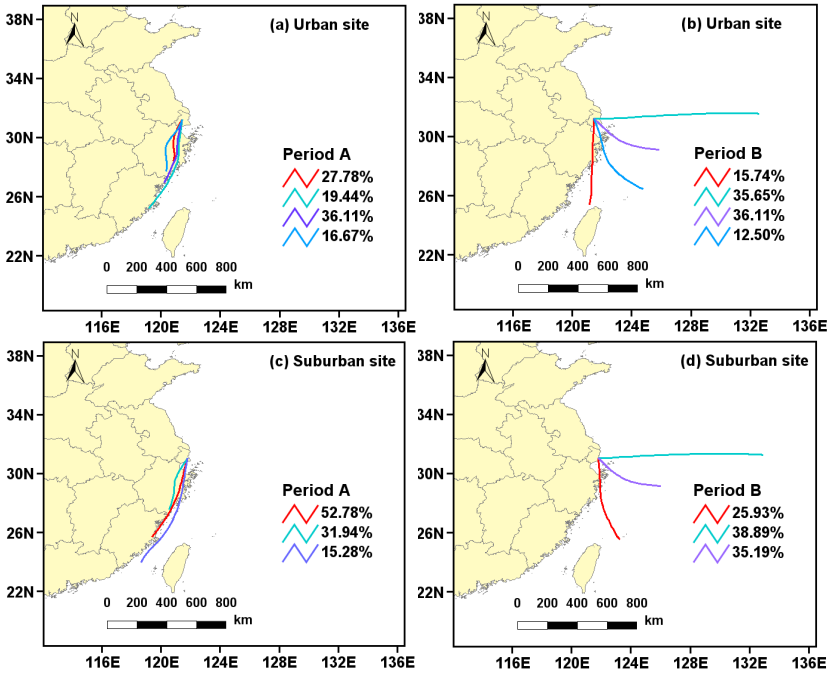

851

852

853 **Figure 3.** Air mass backward trajectories of the major clusters in different periods in

854 the (a–b) urban and (c–d) suburban areas.

855

856

https://doi.org/10.5194/egusphere-2023-1292
Preprint. Discussion started: 14 June 2023

Figure 4.

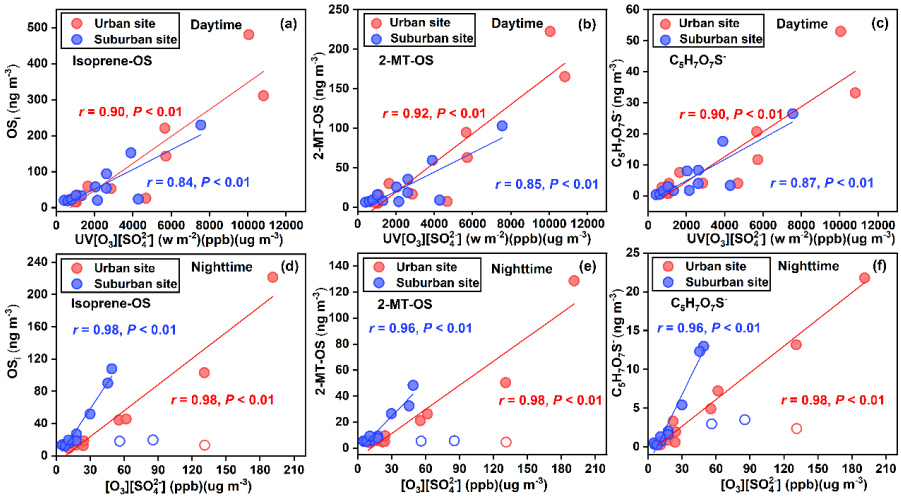

Figure 4. Mass concentrations of (a and d) OS_i, (b and e) 2-MT-OS, and (c and f) $C_5H_7O_7S^-$ as functions of $UV[O_3][SO_4^{2-}]$ and $[O_3][SO_4^{2-}]$ during daytime and nighttime in the urban (red solid circles) and suburban sites (blue solid circles). The open circles represent outliers, which was attributed to several particularly high sulfate events.

https://doi.org/10.5194/egusphere-2023-1292
Preprint. Discussion started: 14 June 2023

865 **Figure 5.**

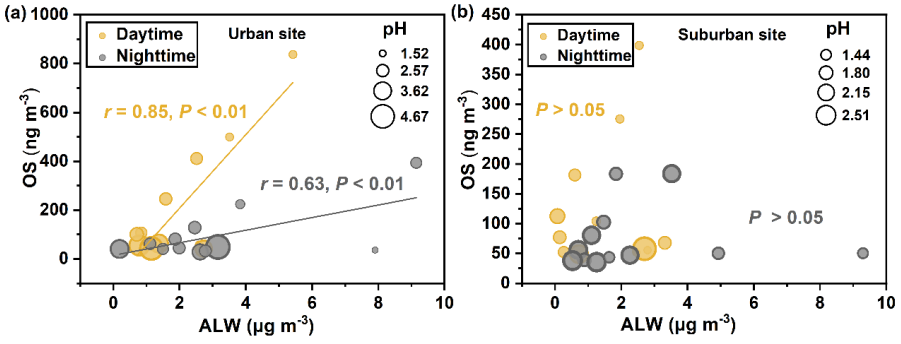

866

867 **Figure 5.** Scatterplots of the ALW concentrations with the mass concentrations of total

868 OSs in $PM_{2.5}$ collected in the (a) urban and (b) suburban areas. Yellow and grey lines

869 show regression lines in the daytime and nighttime, respectively.

870

https://doi.org/10.5194/egusphere-2023-1292
Preprint. Discussion started: 14 June 2023

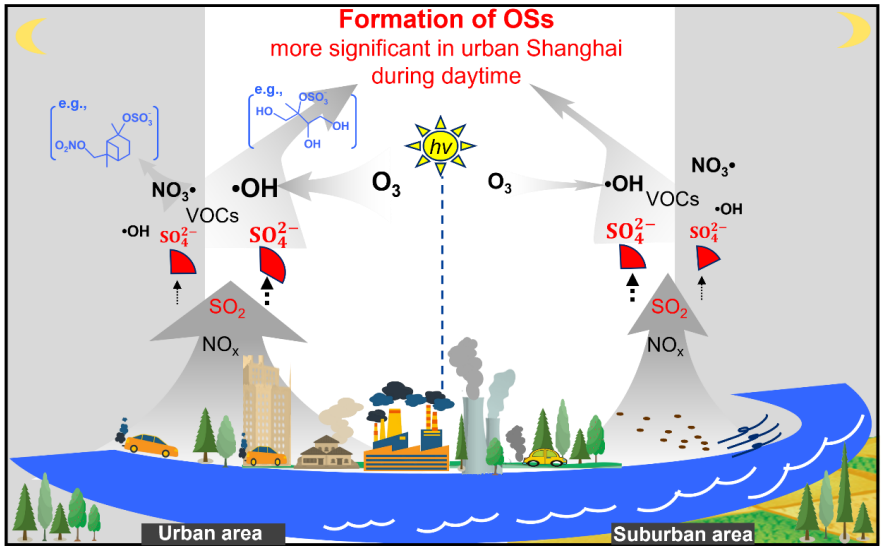

871

872 **Figure 6.** Conceptual picture showing the characteristic and atmospheric process of

873 OSs in urban and suburban Shanghai.

874